Published in final edited form as:
Dev Neurosci. 2007 ; 29(1-2): 113–123.

Citron Kinase is Required for Postnatal Neurogenesis in the Hippocampus

James B. Ackman,
Department of Physiology and Neurobiology, University of Connecticut, Storrs, CT, USA

Raddy L. Ramos,
Department of Physiology and Neurobiology, University of Connecticut, Storrs, CT, USA

Matthew R. Sarkisian, and
Department of Neurobiology, Yale University School of Medicine, New Haven, CT, USA

Joseph J. LoTurco
Department of Physiology and Neurobiology, University of Connecticut, Storrs, CT, USA

Abstract

The dentate gyrus is a site of continual neurogenesis in the postnatal mammalian brain. Here we investigated postnatal neurogenesis in the citron-kinase (citron-K) null mutant rat, *flathead*. The *flathead* rat has substantial deficits in embryonic neurogenesis that are due to failed cytokinesis and cell death. We report here the loss of citron-K function has an even more severe effect on postnatal neurogenesis in the dentate gyrus. Analysis of phosH3 expression in postnatal neurogenic regions of the *flathead* mutant revealed a complete lack of mitotic cells in the dentate gyrus and a large reduction in the number of dividing cells in the *flathead* SVZ. Examination of BrdU incorporation in *flathead* revealed that the *flathead* had a 99% reduction in the number of newly generated cells in the dentate gyrus at postnatal day 10. In addition, doublecortin positive cells were essentially absent from the postnatal *flathead* dentate gyrus which also lacked the vimentin and nestin positive radial glia scaffold that defines the neurogenic niche in postnatal subgranular zone. Together these results indicate that postnatal neurogenesis in the dentate gyrus is eliminated by loss of citron-K function, and suggests that a citron-K dependent progenitor lineage forms the postnatal neuronal progenitor population in the dentate gyrus.

Keywords

neural stem cells; neurogenesis; dentate gyrus; epilepsy

Introduction

Neurogenesis is a continual process in the dentate gyrus of the hippocampus. Generation of dentate granule neurons has been shown to occur in the adult brain of rodents [Altman and Das, 1965; Cameron et al., 1993; Kaplan and Hinds, 1977], primates [Gould et al., 1999; Kornack and Rakic, 1999], and humans [Eriksson et al., 1998]. These newly born dentate granule neurons originate from a pool of neural stem cells present within the subgranular zone (SGZ) of the dentate gyrus [Gage et al., 1995; Palmer et al., 1997; Seri et al., 2001]. Neural stem cells present in neurogenic regions of the adult mammalian brain, including the SGZ and the subventricular zone (SVZ), have been identified as a constituent of the radial glia-astrocyte

Full address Joe LoTurco, Department of Physiology and Neurobiology, Box U-3156, University of Connecticut, Storrs, CT 06269, loturco@uconn.edu, phone: 860-486-3283, fax: 860-486-3303.

lineage [Doetsch et al., 1999; Doetsch et al., 1999; Laywell et al., 2000; Imura et al., 2003; Merkle et al., 2004; Garcia et al., 2004; Seri et al., 2001].

Though neurogenesis occurs in the dentate gyrus throughout life, the peak of dentate granule cell production occurs during the first two weeks of postnatal development in rodents [Bayer, 1980; Schlessinger et al., 1975]. This period of peak neurogenesis occurs following a number of discrete developmental steps that take place during embryonic and postnatal development [Altman and Bayer, 1990a; Altman and Bayer, 1990b; Li and Pleasure, 2005]. Among the initial steps in dentate gyrus development is the migration of the earliest born granule neurons from their place of birth in the neuroepithelium to the dentate gyrus anlage to form the primordial granule cell layer [Altman and Bayer, 1990a; Altman and Bayer, 1990b]. These pioneer granule cells migrate along the radial glia scaffold that extends from the ventricular zone (VZ) to the dentate primordium together with a secondary population of neurogenic progenitors [Altman and Bayer, 1990a; Altman and Bayer, 1990b; Rickmann et al., 1987]. This secondary progenitor population is established in the hilar region of the developing dentate formation during late embryonic development and undergoes a radial transformation to form the SGZ neuroepithelium from which postnatal and adult neurogenesis will originate [Altman and Bayer, 1990a; Altman and Bayer, 1990b; Eckenhoff and Rakic, 1984; Guéneau et al., 1982; Alvarez-Buylla and Lim, 2004].

The *flathead* mutant rat exhibits a CNS specific phenotype that includes severe micrencephaly and frequent seizures [Sarkisian et al., 1999]. The numbers of neurons in the cerebellum, dentate gyrus, olfactory bulb, and upper neocortical layers are dramatically reduced in *flathead* and the brain is 50% smaller than wildtype at birth. Although migration and lamination of the *flathead* neocortex is intact, up to 50% of pyramidal and non-pyramidal neurons are binucleate, indicating a cytokinesis failure during embryonic development [Sarkisian et al., 2001]. In addition, loss of citron kinase function causes deficits in mitosis [LoTurco et al., 2003] and an increase in apoptosis [Di Cunto et al., 2000; Roberts et al., 2000; Sarkisian et al., 2001]. The *flathead* mutation has been identified as a premature stop codon in the first exon of the citron-kinase gene [Sarkisian et al., 2002]. Citron-K is expressed in dividing cells during embryonic development where it localizes to the cleavage furrow of cells undergoing cytokinesis but is absent in the *flathead* mutant [Sarkisian et al., 2002; Di Cunto et al., 2000]. It is hypothesized that citron-K is essential for cytokinesis in neuronogenic divisions, since citron-K is expressed in the developing cerebral cortex during the peak period for generation of late-born cortical neurons, and because many neurons in *flathead* are binucleate whereas glia are not binucleate [LoTurco et al., 2003].

Here, we show that there is a dramatic reduction in the numbers of neurons in the dentate gyrus of *flathead* greater than the decrease in the brain at large. The decrease is associated with a near loss of dividing cells and new neurons in the postnatal DGZ. In comparison, there is a more modest but significant reduction in numbers of dividing cells and neuroblasts in the postnatal SVZ and rostral migratory stream (RMS) of *flathead*. These results demonstrate that postnatal neurogenesis is limited in the SVZ/RMS and virtually absent in the dentate gyrus after loss of citron-K function.

Materials and Methods

Animals and BrdU injections

All animal procedures were performed according to protocols approved by the University of Connecticut Animal Care and Use Committee. *Flathead* mutant rats were obtained from bred colonies at the University of Connecticut. For all experiments, normal littermates from *flathead* litters were used as controls and were designated as wildtype. The normal littermates

included both heterozygous and homozygous wildtype animals. Brains from *flathead* and littermate rats were examined at E14, P0, P7, P14, P16, P17, P19, P21, P22, and P24.

For BrdU injections, pregnant dams received 50 mg/kg BrdU i.p. at 14 and 15 days gestion. Postnatal *flathead* and control pups received 40 mg/kg BrdU i.p. Embryonic rat brains were collected into cold HBSS and fixed overnight in 4% paraformaldehyde (PFA). Postnatal rat pups were euthanized with wet ice (less than P7) or isoflurane (greater than P7) and perfused intracardiallly with PBS followed by 4% PFA. Brains were dissected out and postfixed overnight at 4°C in 4% PFA followed by embedding in 2% agarose. Brains were cut at 40μm on a vibratome (Leica VT-1000S). Free-floating sections were stored at −20°C in cryoprotectant solution (PVP-40, 30% sucrose, in ethylene glycol and 0.2M phosphate buffer, pH 7.4) until use.

Immunocytochemistry, histochemistry, and confocal microscopy

BrdU immunocytochemistry was performed by rinsing free-floating brain sections in PBS followed by denaturation in 2N HCl for 30min at room temperature. Sections were neutralized in 0.1% sodium borate and rinsed in PBS before continuation with the standard immunocytochemistry protocol. The standard immunocytochemistry protocol included blocking sections in 5% donkey serum (Sigma, #D9663) + 0.3% Triton X-100 for 1 hour at room temperature followed by incubation in primary antibodies overnight at 4°C. After rinsing for 1 hour, sections were incubated in secondary antibodies for 1 hour at room temperature followed by a final rinse in PBS, mounted on glass slides, and coverslipped in Prolong Antifade (Molecular Probes). The primary antibodies used were: rat anti-BrdU (1:100, Accurate, #OBT0030), goat anti-doublecortin (1:100, Santa Cruz, #sc-8066), mouse anti-NeuN (1:1000, Chemicon, #MAB377), mouse anti-calbindin D28K (1:1000, Sigma, #C8666), rabbit anti-phospho-Histone H3 (1:500, Chemicon, #06-570), mouse anti-vimentin (1:200, Chemicon, #MAB3400). mouse anti-nestin (1:200, Chemicon, #MAB353), and mouse anti-GFAP (1:200, Sigma, #G3893). The secondary antibodies used were: donkey anti-rabbit Alexa 488 (1:200, Molecular Probes), donkey anti-mouse Alexa 488 (1:200, Molecular Probes), donkey anti-rat Cy3 (1:200, Jackson ImmunoResearch), donkey anti-mouse Alexa 568 (1:200, Molecular Probes), and donkey anti-mouse Cy5 (1:200, Jackson ImmunoResearch). Some sections were counterstained with the nuclear label TO-PRO-3 (Molecular Probes).

For use with non-fluorescent histochemistry, sections were rinsed several times with 2.5% NGS in PBS and then incubated in biotinylated secondary antibodies (biotinylated goat anti-mouse; 1:200, Vector Labs, Burlingame, California) for 2 h at room temperature. Sections were rinsed several times with PBS and incubated for 1 h in an avidin--horseradish peroxidase mixture. Sections were rinsed in PBS and then reacted with 0.05% diaminobenzidine in the presence of 0.0015% H2O2. Sections were collected onto gelatin-coated slides, dried for several hours, and coverslipped with Cytoseal.

For Timm histochemistry, rats were perfused with a sodium sulfide medium (4.76g NaH_2PO_4, 4.68g Na_2S in 400ml dH_20) followed by 4% PFA. Brains were cryoprotected in 30% sucrose and frozen over liquid N2. Sections (20μm) were developed in the dark for 30-60min in a solution containing gum arabic (120ml of 20% stock), citrate buffer (20ml of 2M stock), hydroquinone (60ml of a 5.7% stock), and 0.17g silver nitrate. Sections were dehydrated in ethanol, cleared in xylene and coverslipped with DPX.

Slides were imaged with either a Nikon E400 microscope and Spot camera or with a laser scanning confocal microscope (Leica TCS-SP2; laser lines at 488, 543, 633). Confocal images were acquired at 0.3-1.0 μm per z-section.

Quantification

For quantification of mitotic cells, the number of phosH3 positive cells per sagittal section was counted for the dentate gyrus and the SVZ including first 300μm of RMS from *flathead* (ages P10, P16, and P22) and wildtype (ages P16 and P22). For BrdU quantification, animals aged P17 or P22 that had received BrdU injections at P10 or P19 respectively were used. In the dentate gyrus, the number of BrdU positive cells per sagittal section was counted. For SVZ, confocal images (8-bit indexed color) from sagittal sections were thresholded in Image J with a tolerance of 21 and the polygon selection tool was used to outline the SVZ and first 300μm of RMS. The analyze particles tool with a pixel radius of 3 was used to automatically count the number of BrdU positive cells in the SVZ. Several sections of *flathead* and littermate SVZ were hand counted to confirm the validity of the automatic counting procedure. For both phosH3 and BrdU quantification in dentate and SVZ, the mean and SEM for number of positive cells per section calculated for *flathead* and wildtype. For all conditions, quantification was performed on an average of 13 sagittal sections from the medial extent (range of 0.5 – 2.5 mm from midline). Differences between compared means were determined with the Student's *t* test, with $p < 0.05$ considered significant. For all experiments: N=number of animals, n=number of stained sections.

Results

Granule layer dysgenesis in the flathead dentate gyrus

The brain of the citron-K null mutant, *flathead*, is approximately one-half the size of wildtype at birth. Areas of the central nervous system that undergo significant amounts of late embryonic or postnatal neurogenesis, such as retina, cerebellum, olfactory bulb, and dentate gyrus, are the regions most affected by lack of citron-K function [Di Cunto et al., 2000; Roberts et al., 2000]. The dentate gyrus is markedly reduced in size in *flathead* (Fig. 1A-C). Nissl-stained sagittal and coronal sections of P21 wildtype and *flathead* brain reveal that the inferior blade of the dentate gyrus in missing in *flathead* (Fig. 1B, C). The superior blade of dentate that is present in *flathead* is severely reduced in the dorso-ventral and medio-lateral dimensions. In addition, the *flathead* dentate gyrus is reduced in the rostro-caudal extent. In contrast to the dentate gyrus, the CA3-CA1 pyramidal layers of Ammon's horn are more moderately reduced in size in *flathead* and have no apparent gross disruption in organization. To confirm that the cells remaining in the disrupted granule layer of *flathead* dentate gyrus were granule neurons, we performed calbindin D28k immunocytochemistry on horizontal sections of P21 *flathead* and wildtype hippocampus (Fig 1E). We found that calbindin was expressed by cells in the granule cell layer of *flathead*. Furthermore, we performed Timm's silver sulphide staining on horizontal sections of P14 wildtype and *flathead* hippocampus (Fig. 1D). We found that Timm staining intensely labeled granule cell mossy fiber axons in the hilar region and CA3 pyramidal layer of *flathead* hippocampus in a pattern appropriate for mature dentate granule neurons.

Loss of progenitor cells in postnatal flathead dentate gyrus

Next we determined whether proliferating cells were present in the subgranular zone of the *flathead* dentate gyrus using phosphorylated histone H3 (phosH3) and 5-bromodeoxyuridine (BrdU) immunocytochemistry (Fig. 2). There was a lack of phosH3 positive dividing cells in the *flathead* dentate gyrus at P16 and P22 (Fig. 2A, B, F). The number of phosH3 positive cells per section in *flathead* was reduced by 97% with respect to wildtype (0.3 ± 0.1; N=4, n=19 for *flathead*; 8.8 ± 2.9; N=2, n=5 for wildtype; $p < 0.05$). Consistent with a lack of proliferating cells in the dentate gyrus, the number of cells in the P17 *flathead* dentate gyrus that incorporated BrdU at P10 was reduced by 99% (Fig. 2C, D, G) (3.5 ± 0.9 cells/section, N=7, n=11 for *flathead*; 364.3 ± 32.0 cells/section, N=7, n=18 for wildtype; $p < 0.001$).

Next we tested if dentate granule neurons in *flathead* were generated during embryonic development. Consistent with an embryonic birth date, we found that granule neurons in P19 *flathead* dentate gyrus were labelled by BrdU administered at E14 and E15 (Fig. 2E; N=1). Note the presence several binucleate NeuN+ cells near the internal limb of the dentate gyrus (arrowheads, Fig. 2E).

Decreased proliferation in the SVZ and RMS of flathead

Since the SVZ/RMS is a postnatal neurogenic region, we tested for expression of the immature neuron marker, doublecortin in the SVZ/RMS of *flathead*. Doublecortin expression was reduced in the SVZ and RMS of *flathead* at P22 (Fig. 3A). Next we determined whether there was a decrease in the numbers of mitotic progenitors in the SVZ/RMS of *flathead*. Analysis of phosH3 immunocytochemistry on sagittal sections of P22 *flathead* brain revealed that the number of phosH3 expressing cells per section was reduced by 92% in the *flathead* SVZ/RMS (Fig. 3B, D) (11.8 ± 1.7 cells/section, N=4, n=19 for *flathead*; 146.8 ± 26.9 cells/section, N=2, n=4 for wildtype; $p < 0.05$). BrdU immunocytochemistry on sections from P17 animals that received BrdU at P10 confirmed a reduction in newly generated cells in the *flathead* SVZ/RMS (Fig. 3C, E). The decrease in BrdU labeled cells per section was 83% in the *flathead* SVZ/RMS (179.4 ± 39.8 cells/section, N=5, n=15 for *flathead*; 1059.7 ± 113.2 cells/section, N=4, n=9 for wildtype; $p < 0.001$).

Altered neurogenic niche in the flathead dentate gyrus

Next we assessed whether doublecortin expressing cells were present in the postnatal *flathead* dentate gyrus. In contrast to wildtype where there was doublecortin immunoreactivity throughout the dentate gyrus at P17 and P22, most immunostained sections from *flathead* contained no doublecortin positive (DCX+) cells or fibers (Fig. 4A, B) (0.39 ± 0.29 cells/section, N=8, n=23 for *flathead*; N=3, n=8 for wildtype). In the few sections of *flathead* hippocampus where isolated DCX immunoreactivity was present, the positive cells were located in the hilar region between the dentate horn and CA3 (Fig. 4B), whereas DCX+ cells were never found outside the granule cell layer or subgranular zone in wildtype dentate gyrus. In sagittal stained sections the dendrites of hilar DCX+ cells in *flathead* were generally oriented in the caudal or ventral directions towards the dentate molecular layer.

The postnatal SGZ of the dentate gyrus contains radial-type astrocytes that originate from radial glia during development [Eckenhoff and Rakic, 1984; Rickmann et al., 1987]. Radial-type astrocytes generate granule neurons in the dentate gyrus [Seri et al., 2004] and express the intermediate filament proteins vimentin, nestin, and GFAP [Eckenhoff and Rakic, 1984; Rickmann et al., 1987; Lendahl et al., 1990; Seri et al., 2004]. To determine whether radial-type astrocytes were present in the postnatal *flathead* SGZ, we performed vimentin, nestin, and GFAP immunocytochemistry on sagittal sections of wildtype and *flathead* dentate gyrus at P21-P24. The postnatal *flathead* dentate gyrus lacked vimentin and nestin positive radial fibers (Fig. 4C, D) and contained few GFAP positive radial fibers (arrows in Fig. 4E). In contrast to the reduction in radial-type astrocytes, multipolar astrocytes that expressed GFAP were abundant in the *flathead* SGZ, as well as in the hilus and in the molecular layer. In other postnatal neurogenic regions, such as the SVZ/RMS, both radial glia and multipolar-type astrocytes that had intense staining for vimentin, nestin, and GFAP were present in *flathead* (data not shown).

Reduced migration of dentate precursors during development of the flathead dentate gyrus

Next we examined the cytoarchitecture of germinative matrices associated with development of the dentate gyrus. The hippocampal neuroepithelium is established along the medial wall of the lateral ventricle during embryonic development (Fig. 5A). An indentation of the hippocampal neuroepithelium, the dentate notch, is the location of the primary dentate

neuroepithelium from which the earliest generated granule cells originate as well as migrating progenitors that establish the secondary dentate matrix. We analyzed Nissl stained coronal sections of hippocampal neuroepithelium at E14 to see if any gross cytoarchitectural abnormalities were present in the primary dentate neuroepithelium of *flathead* before formation of the secondary dentate matrix. No distinct alterations were present in the primary dentate neuroepithelium of *flathead* at E14 (Fig. 5B). The secondary dentate matrix is a germinative matrix located adjacent to the VZ of the dentate neuroepithelium and becomes evident around E18 in rat [Altman and Bayer, 1990a]. The secondary dentate matrix consists of proliferative cells and migratory cells and extends tangentially towards the dentate gyrus as a subpial migration. This dentate migration is robust during late embryonic and early postnatal development (E20-P5 in rat) [Altman and Bayer, 1990a;Altman and Bayer, 1990b] and contains neuroblasts that migrate to the granule cell layer and progenitors that migrate to establish the proliferative tertiary dentate matrix in the hilus (Fig. 5C). We examined the dentate migration in the perinatal hippocampus, a time during which there are large numbers of cells migrating towards the dentate gyrus. Nissl stained horizontal sections of P0 *flathead* and wildtype hippocampus revealed that the dentate migration in *flathead* is distinctly reduced (Fig. 5D). In addition, there appeared to be a lack of cells aggregating in the region of the internal dentate blade in *flathead*, as well as an areal reduction in the region of the tertiary dentate matrix. In contrast to the dentate migration, which appeared thin between the pial surface and CA3 (boxed area in Fig. 5D), the SVZ, Ammon's horn, stratum radiatium, and the fimbria did not appear particularly reduced in *flathead* at P0. Additionally, we observed an increased number of pyknotic nuclei in Nissl stained sections at P0 in the secondary dentate matrix, the dentate migration, and the tertiary matrix in *flathead* (data not shown). Increased cell death in the dentate germinative matrices is consistent with previous studies indicating that lack of citron-K function leads to failed cytokinesis and massive apoptosis in germinal zones such as the ganglionic eminence, neocortical VZ/SVZ, and the cerebellar granule layer [Roberts et al., 2000;Sarkisian et al., 2001;Di Cunto et al., 2000]. By P7 the density of cells in the dentate migration has decreased in both wildtype and *flathead* (Fig. 5E). Notice that by P7 the dentate gyrus has greatly increased in size and the internal blade of the dentate gyrus has formed in wildtype, whereas in *flathead* the dentate has not undergone a similar increase in size and the internal blade is mostly absent.

Discussion

Previous studies have demonstrated severe deficits in embyronic neurogenesis and increased apoptosis in citron-K null mutants [Di Cunto et al., 2000; Roberts et al., 2000; Sarkisian et al., 2002]. Here, we show that postnatal neurogenesis is depleted in the citron-K null mutant rat, *flathead*. The depletion of postnatal neurogenesis in *flathead* can most likely be attributed to a loss of mitotic progenitors in postnatal neurogenic regions as proliferation was decreased in the SVZ/RMS and nearly completely absent in the dentate gyrus. These results indicate that citron-K function is required for development of the neurogenic progenitor pool in the postnatal dentate gyrus.

Among the developmental steps required for formation of the dentate gyrus is the establishment of a tertiary progenitor population in the SGZ during late embryonic and early postnatal development (also termed the “tertiary germinative matrix”; see Altman and Bayer 1990a, b). It seems likely from our results that the tertiary precursor pool fails to be established in the dentate gyrus of the citron-K null mutant, *flathead* as there was a lack mitotic progenitors in the SGZ, as well as a lack of newly generated neurons in the granule cell layer of postnatal *flathead* hippocampus. In addition, radial-type astrocytes were absent in the postnatal *flathead* SGZ. Since radial-type astrocytes serve as progenitors of new granule neurons in the adult dentate gyrus [Seri et al., 2004], these results indicate that formation of the neurogenic niche is disrupted in the *flathead* SGZ.

Though there was a lack of neurogenesis in the postnatal *flathead* dentate gyrus, granule cells were present in the rudimentary granule layer of *flathead*. These *flathead* granule cells possessed key differentiated granule neuron characteristics such as calbindin expression and Timm staining of mossy fiber axons. In addition, granule cells that were present in the *flathead* dentate gyrus were found to incorporate BrdU administered at E14-E15, a time during which only the primordial granule neuron population is being generated. The presence of a rudimentary granule cell layer consisting of early-born granule neurons in *flathead*, indicates that the disruption in dentate gyrus development is fundamentally different from other rodent models involving deficits in SGZ precursor pool establishment such as Wnt signaling and CXCR4 mutants where the dentate gyrus completely fails to form [Galceran et al., 2000; Lee et al., 2000; Zhou et al., 2004; Bagri et al., 2002; Lu et al., 2002]. These results indicate that early in development generation and migration of the pioneer granule neurons into the dentate anlage can occur in absence of citron-K function but that the subsequent progenitor-progenitor or progenitor-neuron divsions from which the majority of granule neuron originate require citron-K function.

Exactly how citron-K function is involved in development of the SGZ progenitor population is not known. During embyronic development, citron-K is expressed in a portion of dividing progenitors along the VZ surface resulting in about half of cortical neurons being multinucleate due to cytokinesis failure [Sarkisian et al., 2002]. Study of the postnatal brain with *in situ* hybridization has revealed that citron-K message is expressed in the external granule layer of the cerebellum as well as in the SVZ and RMS of the forebrain [Di Cunto et al., 2000]. Although citron-K expresssion has not been reported in the postnatal dentate gyrus, it possible that it is present at low levels and that lack of citron-K function leads to progenitor cell depletion in the SGZ due to cytokinesis failure and apoptosis. Alternatively, lack of citron-K function could cause progenitor cell depletion in the hippocampal neuroepithelium, before the tertiary precursor population migrates into the hilus and SGZ. Our results showing a diminished dentate migration from the secondary germinative matrix to the dentate formation indicates that lack of citron-K function may deplete progenitors and neuroblasts before their migration into the hilus and the granule cell layer.

Citron-K mutants exhibit frequent seizures that begin near the end of the first postnatal week [Sarkisian et al., 1999; Di Cunto et al., 2000]. Temporal lobe epilepsy is often associated with disorganization or loss of cells in the granule cell layer of dentate gyrus [Houser, 1990; Houser, 1992]. It seems possible that frequent seizure activity may have a detrimental effect on development of the *flathead* dentate gyrus. However, it seems unlikely that the frequent seizures in *flathead* would cause the loss of the SGZ progenitor population. First, seizures in *flathead* start at the end of the first postnatal week, after the secondary progenitor population has migrated to and become established in the SGZ/hilus [Sarkisian et al., 1999]. Second, seizure activity has been reported to increase granule neuron neurogenesis in the dentate gyrus [Parent et al., 1997]. Although the results presented here did not include analysis of BrdU incorportation in the postnatal *flathead* brain earlier than the first postnatal week, we have examined BrdU incorporation at P2 in *flathead* and found that the lack of dentate granule neuron generation was present at this early postnatal age as well (data not shown). We have not assessed proliferation at this early postnatal age with mitotic markers or short survival BrdU assays, but examination of neonatal *flathead* hippocampus with Nissl staining indicates that the morphological abnormalities in dentate gyrus development are present in the *flathead* within the first posntatal week. In conclusion, postnatal neurogenesis in the dentate gyrus is dependent upon citron-K function, and as there is an apparent loss of dividing cells in postnatal DGZ we further suggest that citron-K function is required for production of the SGZ progenitor population from earlier, perhaps fetal, progenitors.

Acknowledgements

Work was supported by NIH grant MH056524 to JJL.

References

Altman J, Bayer SA. Mosaic organization of the hippocampal neuroepithelium and the multiple germinal sources of dentate granule cells. J Comp Neurol 1990;301:325–42. [PubMed: 2262594]

Altman J, Bayer SA. Migration and distribution of two populations of hippocampal granule cell precursors during the perinatal and postnatal periods. J Comp Neurol 1990;301:365–81. [PubMed: 2262596]

Altman J, Das GD. Autoradiographic and histological evidence of postnatal hippocampal neurogenesis in rats. J Comp Neurol 1965;124:319–35. [PubMed: 5861717]

Alvarez-Buylla A, Lim DA. For the long run: maintaining germinal niches in the adult brain. Neuron 2004;41:683–6. [PubMed: 15003168]

Bagri A, Gurney T, He X, Zou YR, Littman DR, Tessier-Lavigne M, Pleasure SJ. The chemokine SDF1 regulates migration of dentate granule cells. Development 2002;129:4249–60. [PubMed: 12183377]

Bayer SA. Development of the hippocampal region in the rat. I. Neurogenesis examined with 3H-thymidine autoradiography. J Comp Neurol 1980;190:87–114. [PubMed: 7381056]

Cameron HA, Woolley CS, McEwen BS, Gould E. Differentiation of newly born neurons and glia in the dentate gyrus of the adult rat. Neuroscience 1993;56:337–44. [PubMed: 8247264]

Di Cunto F, Imarisio S, Hirsch E, Broccoli V, Bulfone A, Migheli A, Atzori C, Turco E, Triolo R, Dotto GP, Silengo L, Altruda F. Defective neurogenesis in citron kinase knockout mice by altered cytokinesis and massive apoptosis. Neuron 2000;28:115–27. [PubMed: 11086988]

Doetsch F, Caille I, Lim DA, Garcia-Verdugo JM, Alvarez-Buylla A. Subventricular zone astrocytes are neural stem cells in the adult mammalian brain. Cell 1999;97:703–16. [PubMed: 10380923]

Doetsch F, Garcia-Verdugo JM, Alvarez-Buylla A. Regeneration of a germinal layer in the adult mammalian brain. Proc Natl Acad Sci U S A 1999;96:11619–24. [PubMed: 10500226]

Eckenhoff MF, Rakic P. Radial organization of the hippocampal dentate gyrus: a Golgi, ultrastructural, and immunocytochemical analysis in the developing rhesus monkey. J Comp Neurol 1984;223:1–21. [PubMed: 6707248]

Eriksson PS, Perfilieva E, Bjork-Eriksson T, Alborn AM, Nordborg C, Peterson DA, Gage FH. Neurogenesis in the adult human hippocampus. Nat Med 1998;4:1313–7. [PubMed: 9809557]

Gage FH, Coates PW, Palmer TD, Kuhn HG, Fisher LJ, Suhonen JO, Peterson DA, Suhr ST, Ray J. Survival and differentiation of adult neuronal progenitor cells transplanted to the adult brain. Proc Natl Acad Sci U S A 1995;92:11879–3. [PubMed: 8524867]

Galceran J, Miyashita-Lin EM, Devaney E, Rubenstein JL, Grosschedl R. Hippocampus development and generation of dentate gyrus granule cells is regulated by LEF1. Development 2000;127:469–82. [PubMed: 10631168]

Garcia AD, Doan NB, Imura T, Bush TG, Sofroniew MV. GFAP-expressing progenitors are the principal source of constitutive neurogenesis in adult mouse forebrain. Nat Neurosci 2004;7:1233–41. [PubMed: 15494728]

Gould E, Reeves AJ, Fallah M, Tanapat P, Gross CG, Fuchs E. Hippocampal neurogenesis in adult Old World primates. Proc Natl Acad Sci U S A 1999;96:5263–7. [PubMed: 10220454]

Guéneau G, Privat A, Drouet J, Court L. Subgranular zone of the dentate gyrus of young rabbits as a secondary matrix. A high-resolution autoradiographic study. Dev Neurosci 1982;5:345–58. [PubMed: 7140583]

Houser CR. Granule cell dispersion in the dentate gyrus of humans with temporal lobe epilepsy. Brain Res 1990;535:195–204. [PubMed: 1705855]

Houser CR. Morphological changes in the dentate gyrus in human temporal lobe epilepsy. Epilepsy Res Suppl 1992;7:223–34. [PubMed: 1466768]

Imura T, Kornblum HI, Sofroniew MV. The predominant neural stem cell isolated from postnatal and adult forebrain but not early embryonic forebrain expresses GFAP. J Neurosci 2003;23:2824–32. [PubMed: 12684469]

Kaplan MS, Hinds JW. Neurogenesis in the adult rat: electron microscopic analysis of light radioautographs. Science 1977;197:1092–4. [PubMed: 887941]

Kornack DR, Rakic P. Continuation of neurogenesis in the hippocampus of the adult macaque monkey. Proc Natl Acad Sci U S A 1999;96:5768–3. [PubMed: 10318959]

Laywell ED, Rakic P, Kukekov VG, Holland EC, Steindler DA. Identification of a multipotent astrocytic stem cell in the immature and adult mouse brain. Proc Natl Acad Sci U S A 2000;97:13883–8. [PubMed: 11095732]

Lee SM, Tole S, Grove E, McMahon AP. A local Wnt-3a signal is required for development of the mammalian hippocampus. Development 2000;127:457–67. [PubMed: 10631167]

Lendahl U, Zimmerman LB, McKay RD. CNS stem cells express a new class of intermediate filament protein. Cell 1990;60:585–95. [PubMed: 1689217]

Li G, Pleasure SJ. Morphogenesis of the dentate gyrus: what we are learning from mouse mutants. Dev Neurosci 2005;27:93–9. [PubMed: 16046842]

LoTurco JJ, Sarkisian MR, Cosker L, Bai J. Citron kinase is a regulator of mitosis and neurogenic cytokinesis in the neocortical ventricular zone. Cereb Cortex 2003;13:588–91. [PubMed: 12764032]

Lu M, Grove EA, Miller RJ. Abnormal development of the hippocampal dentate gyrus in mice lacking the CXCR4 chemokine receptor. Proc Natl Acad Sci U S A 2002;99:7090–5. [PubMed: 11983855]

Merkle FT, Tramontin AD, García-Verdugo JM, Alvarez-Buylla A. Radial glia give rise to adult neural stem cells in the subventricular zone. Proc Natl Acad Sci U S A 2004;101:17528–32. [PubMed: 15574494]

Palmer TD, Takahashi J, Gage FH. The adult rat hippocampus contains primordial neural stem cells. Mol Cell Neurosci 1997;8:389–404. [PubMed: 9143557]

Parent JM, Yu TW, Leibowitz RT, Geschwind DH, Sloviter RS, Lowenstein DH. Dentate granule cell neurogenesis is increased by seizures and contributes to aberrant network reorganization in the adult rat hippocampus. J Neurosci 1997;17:3727–38. [PubMed: 9133393]

Rickmann M, Amaral DG, Cowan WM. Organization of radial glial cells during the development of the rat dentate gyrus. J Comp Neurol 1987;264:449–79. [PubMed: 3680638]

Roberts MR, Bittman K, Li WW, French R, Mitchell B, LoTurco JJ, D'Mello SR. The flathead mutation causes CNS-specific developmental abnormalities and apoptosis. J Neurosci 2000;20:2295–306. [PubMed: 10704505]

Sarkisian M, Rattan S, D'Mello S, LoTurco J. Characterization of seizures in the flathead rat: a new genetic model of epilepsy in early postnatal development. Epilepsia 1999;40:394–400. [PubMed: 10219263]

Sarkisian MR, Frenkel M, Li W, Oborski JA, LoTurco JJ. Altered interneuron development in the cerebral cortex of the flathead mutant. Cereb Cortex 2001;11:734–43. [PubMed: 11459763]

Sarkisian MR, Li W, Di Cunto F, D'Mello SR, LoTurco JJ. Citron-kinase, a protein essential to cytokinesis in neuronal progenitors, is deleted in the flathead mutant rat. J Neurosci 2002;22:RC217. [PubMed: 11932363]

Schlessinger AR, Cowan WM, Gottlieb DI. An autoradiographic study of the time of origin and the pattern of granule cell migration in the dentate gyrus of the rat. J Comp Neurol 1975;159:149–75. [PubMed: 1112911]

Seri B, Garcia-Verdugo JM, McEwen BS, Alvarez-Buylla A. Astrocytes give rise to new neurons in the adult mammalian hippocampus. J Neurosci 2001;21:7153–60. [PubMed: 11549726]

Seri B, García-Verdugo JM, Collado-Morente L, McEwen BS, Alvarez-Buylla A. Cell types, lineage, and architecture of the germinal zone in the adult dentate gyrus. J Comp Neurol 2004;478:359–78. [PubMed: 15384070]

Zhou CJ, Zhao C, Pleasure SJ. Wnt signaling mutants have decreased dentate granule cell production and radial glial scaffolding abnormalities. J Neurosci 2004;24:121–6. [PubMed: 14715945]

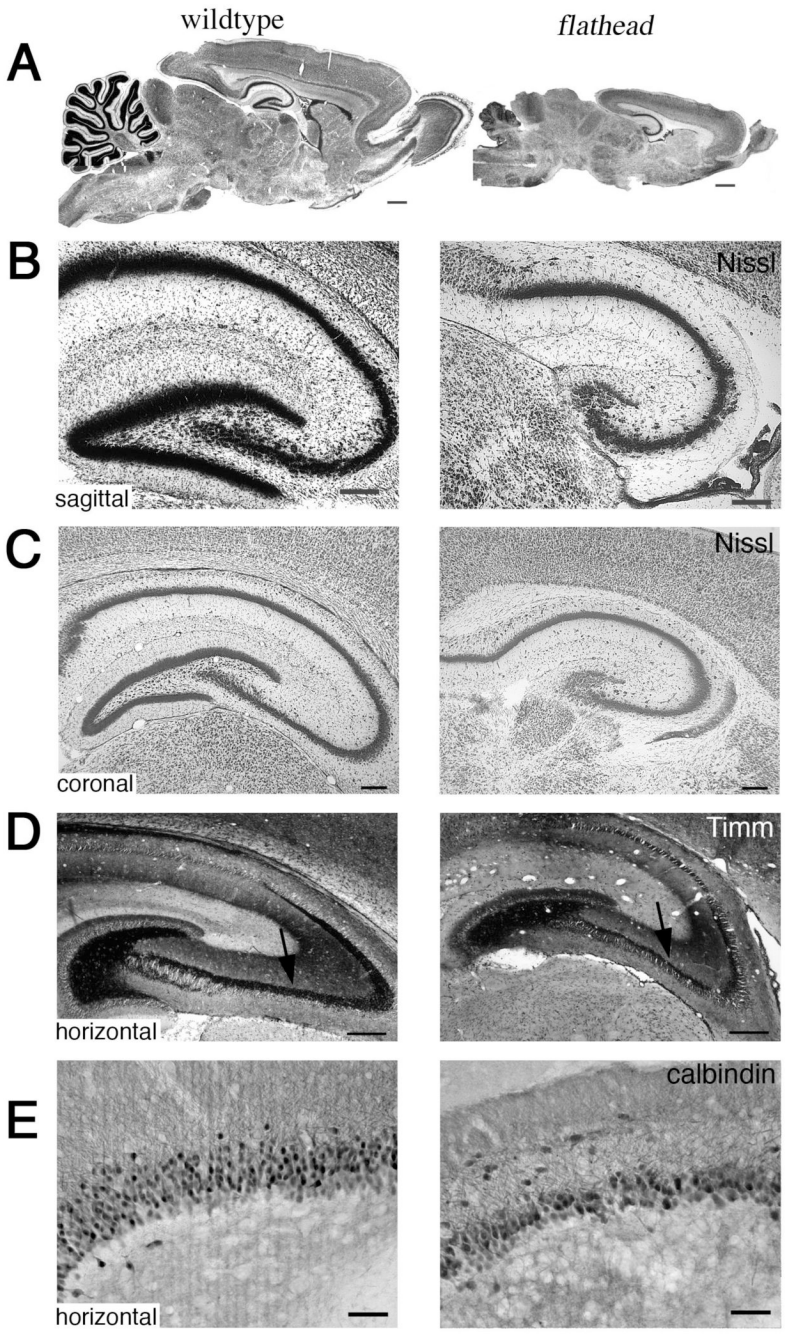

Figure 1. Dysgenesis of the granule cell layer in the *flathead* dentate gyrus

(**A**) Nissl stained sagittal sections of wildtype and *flathead* brains at P21. (**B**) Higher magnification comparison of Nissl staining in sagittal sections of wildtype and *flathead* hippocampus. (**C**) Higher magnification comparison of Nissl staining in coronal sections of P21 wildtype and *flathead* hippocampus. (**D**) Timm staining of granule cell mossy fiber axons (arrows) in horizontal sections of P14 wildtype and *flathead* hippocampus. (**E**) Expression of calbindin in horizontal sections of P21 wildtype and *flathead* dentate gyrus. In the images, medial is down and rostral is to the right. Scale bars: A, 1mm; B-E, 250μm.

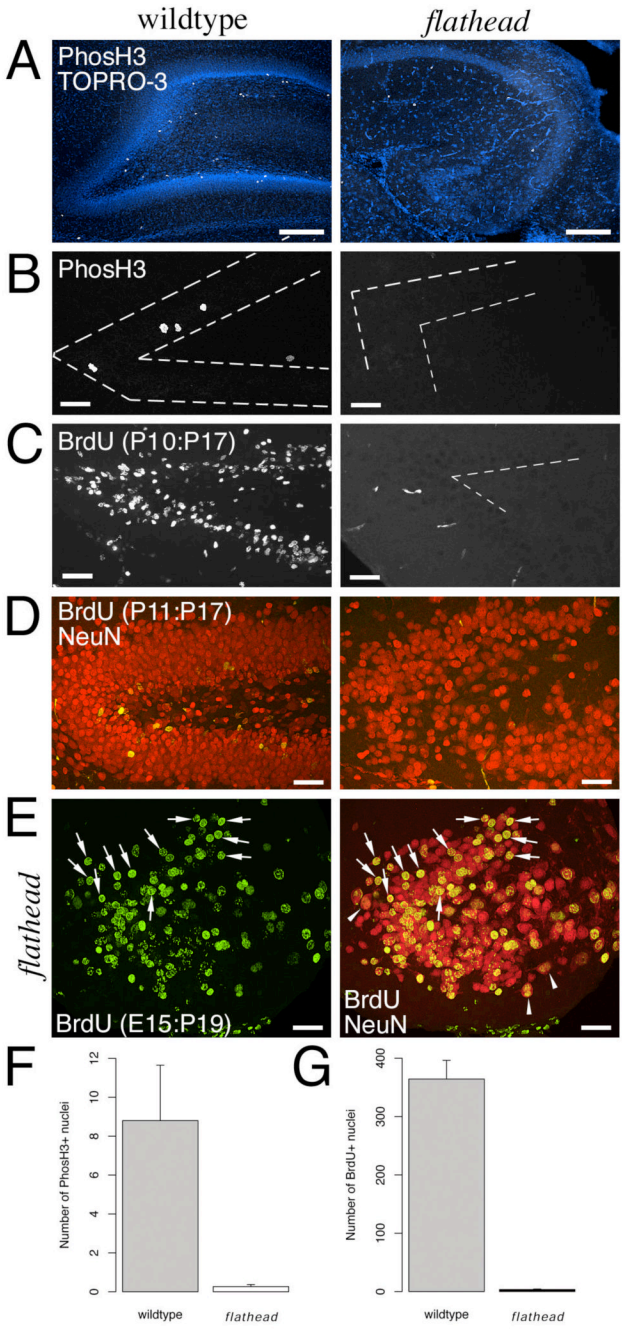

Figure 2. Proliferating cells are absent in the postnatal *flathead* dentate gyrus

(**A**) Lack of PhosH3+ nuclei (white) in *flathead* subgranular zone (SGZ) at P16. Section is counterstained with the nuclear label TO-PRO-3 (blue). (**B**) Lack of PhosH3+ nuclei in *flathead* SGZ at P22. Dashed lines outline the granule cell layer. (**C**) Decreased numbers of BrdU+ cells in the postnatal *flathead* dentate gyrus. The images are from P17 wildtype and *flathead* animals that received BrdU injections at P10. The few BrdU positive objects next to the dentate gyrus in this image are blood vessels. **(D)** Lack of newly generated granule neurons in the *flathead* dentate gyrus. BrdU is green and NeuN is red. (**E**) Dentate granule neurons in *flathead* incorporate BrdU at E14-E15 (arrows). Image is from a P19 *flathead* that received BrdU on E14 and E15. Binucleate neurons are indicated by arrowheads. **(F)** Quantification of

PhosH3+ nuclei in the SGZ. Numbers are expressed as the mean number of PhosH3+ cells in the SGZ per section. $p < 0.05$. **(G)** Quantification of the number of BrdU+ cells in the dentate gyrus. Numbers are expressed as mean number of BrdU+ nuclei per section. $p < 0.001$. Scale bars: A-E, 40μm.

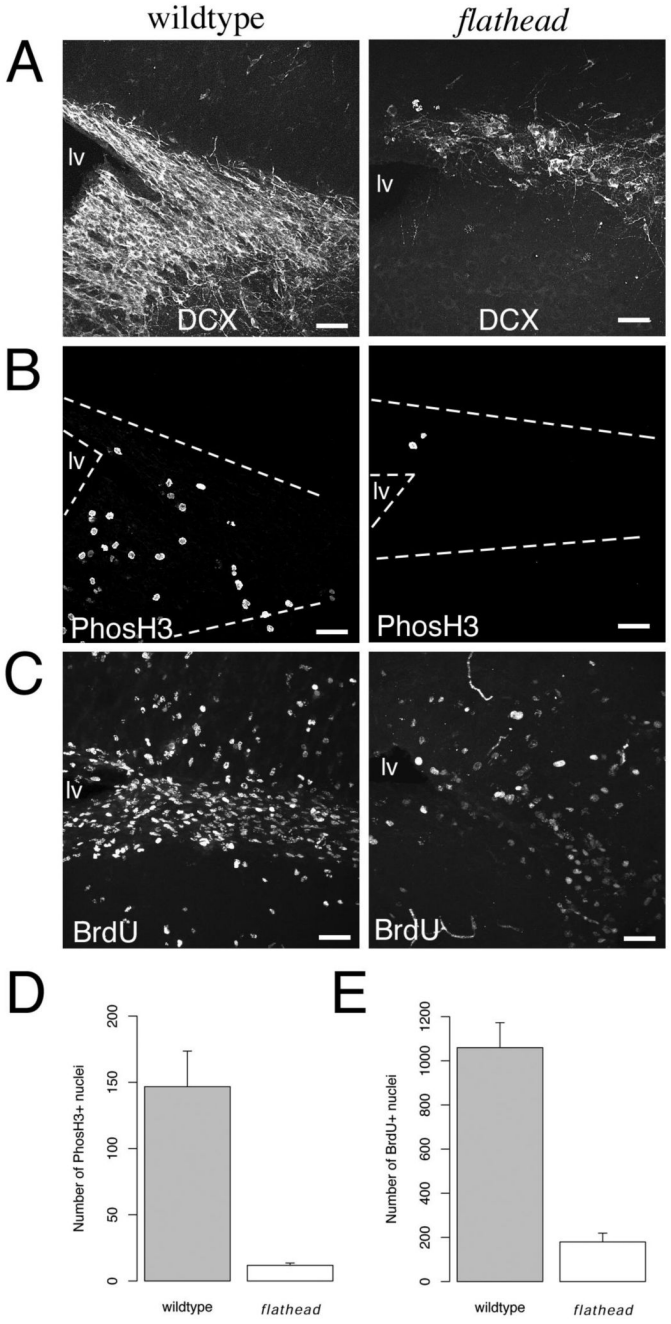

Figure 3. Decreased proliferation in the postnatal subventricular zone of the *flathead* rat

(**A**) Expression of doublecortin and PhosH3 in the SVZ of wildtype and *flathead* rat at P22. (**B**) Reduced numbers of PhosH3+ nuclei in the *flathead* SVZ at P22. The images are from the same sections shown in **A**. (**C**) Decreased numbers of BrdU+ cells in the postnatal *flathead* SVZ. The images are from P17 wildtype and *flathead* animals that received BrdU injections at P10. **(D)** Quantification of PhosH3+ nuclei in the SVZ. Numbers are expressed as the mean number of PhosH3+ cells in the SVZ per section. $p < 0.05$. **(E)** Quantification of the number newly generated cells in the SVZ. Numbers are expressed as the mean number of BrdU+ nuclei in the SVZ. $p < 0.001$. Scale bars: A-C, 40μm.

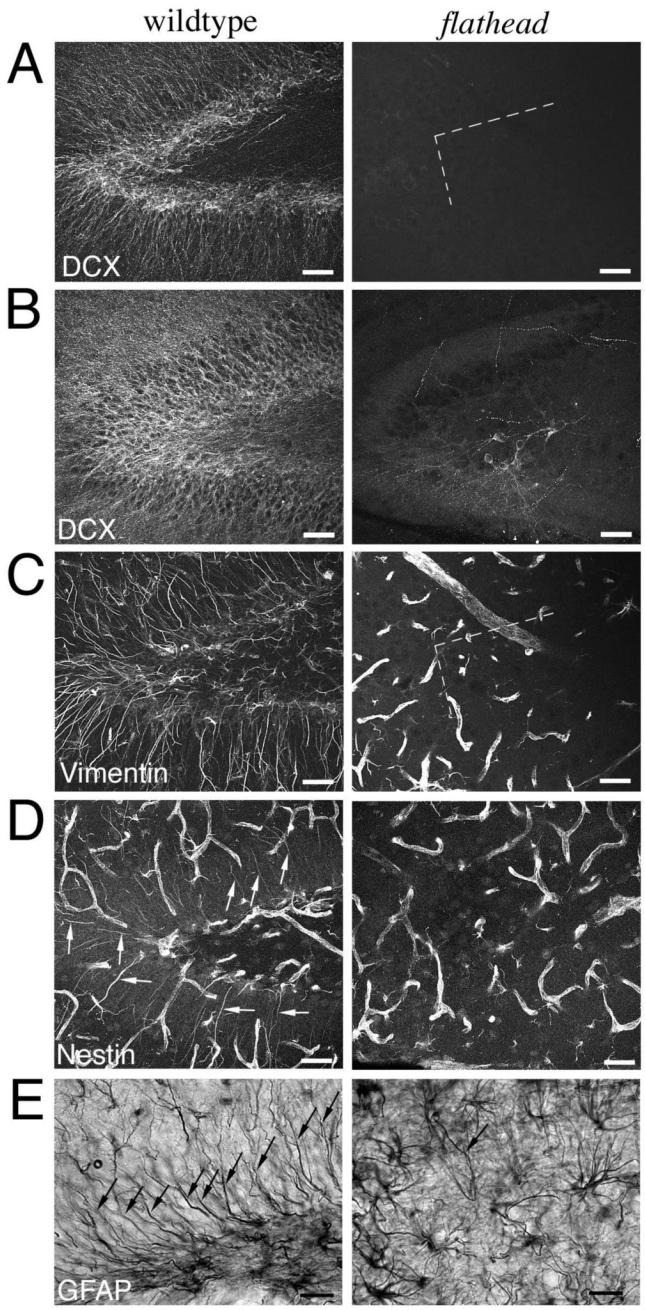

Figure 4. Altered neurogenic niche in the *flathead* dentate gyrus

(**A**) Doublecortin expression in wildtype and *flathead* dentate gyrus at P17. Notice the dramatic reduction in doublecortin+ cells and processes within the dentate granule cell layer of the *flathead*. (**B**) Doublecortin expression in the dentate gyrus of wildtype and *flathead* rat at P22. (**C**) Vimentin expression in the dentate gyrus of wildtype and *flathead* rat at P22. Notice the high density of vimentin+ radial fibers in wildtype dentate and the lack of radial fibers in *flathead*. (**D**) Nestin expression in the dentate gyrus of wildtype and *flathead* rat at P24. Nestin expression was located in endothelial cells, multipolar astrocytes, and radial-type astrocytes in the wildtype dentate gyrus, whereas in the *flathead* dentate gyrus only nestin+ endothelial cells and multipolar astrocytes were found. Arrows indicate examples of nestin+ radial fibers

in wildtype dentate gyrus. (**E**) GFAP immunohistochemistry in the dentate gyrus of wildtype and *flathead* rat at P21. Notice the lack of GFAP+ radial fibers in the *flathead* dentate gyrus. Arrows indicate GFAP+ radial fibers. Scale bars: A-D, 40μm; E, 25μm.

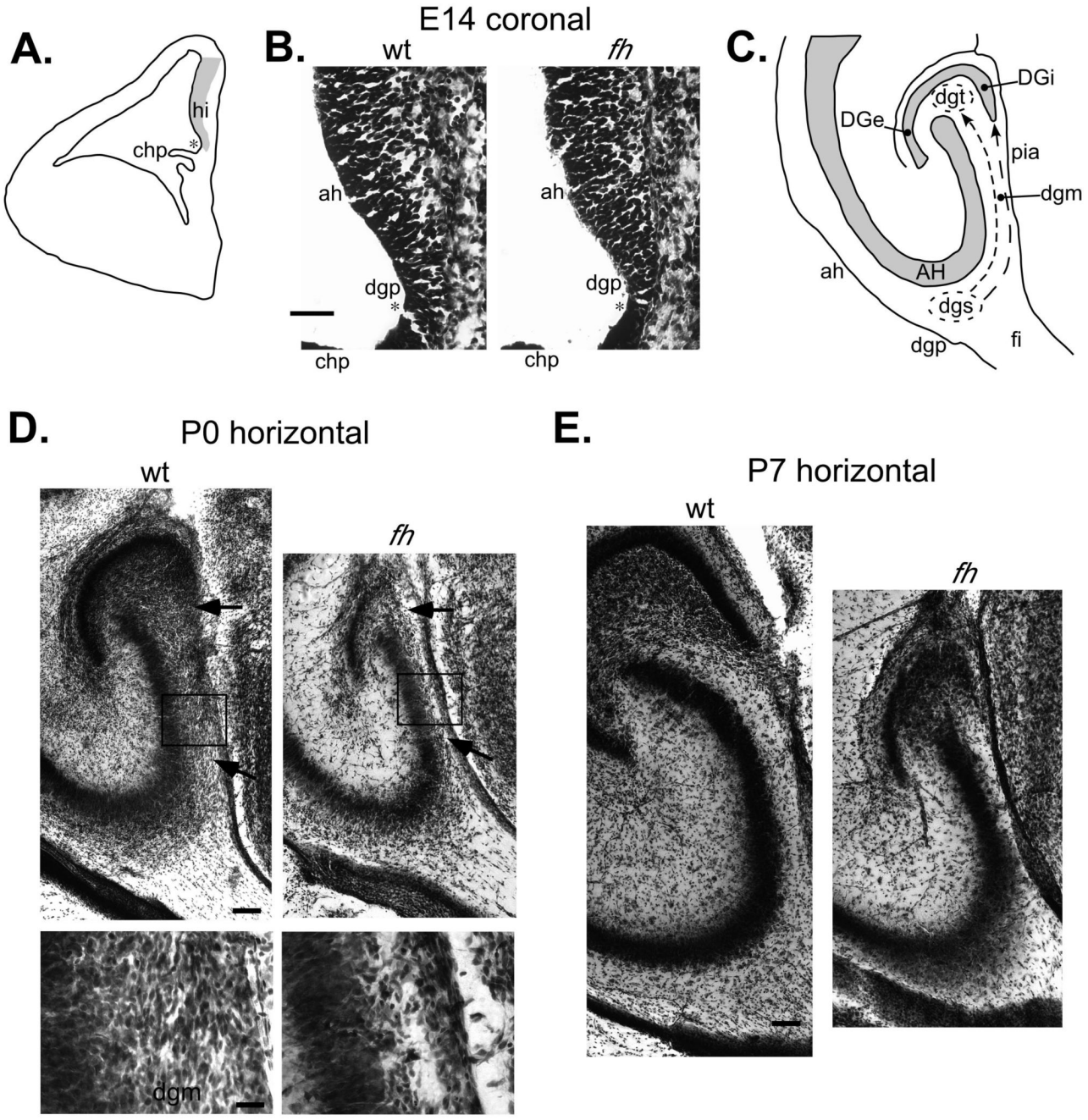

Figure 5. Diminished dentate migratory stream during development of the *flathead* dentate gyrus

(**A**) Location of hippocampal neuroepithelium (hi) in the developing rat brain. Dentate notch indicated by asterisk; Choroid plexus, chp. (**B**) Nissl stained coronal sections of wildtype and *flathead* hippocampal neuroepithelium at E14. Note the similarity in appearance between wildtype and *flathead* Ammonic neuroepithelium (ah) and primary dentate neuroepithelium (dgp). (**C**) Overview of dentate gyrus development during the late embryonic and early postnatal periods. The dentate migratory stream (dgm) consists of neuroblasts and progenitors which migrate to form the internal blade of the dentate gyrus (DGi) and the proliferative tertiary dentate matrix (dgt) in the hilus. Ammon's horn, AH; External blade of the dentate gyrus, DGe; fimbria, fi; secondary dentate matrix, dgs. (**D**) Nissl stained horizontal sections of wildtype

and *flathead* hippocampus at P0. Note the decreased number of cells in the *flathead* dgm compared with the wildtype dgm (arrows). The panel of high magnification dgm images below were taken from the region outlined by the boxes in the upper panel. (**E**) Nissl stained horizontal sections of wildtype and *flathead* hippocampus at P7. Scale bars: B, 50μm; D upper panel, 100μm; D lower panel, 25μm; E, 100μm.